HHS Public Access

Author manuscript

Biomater Sci. Author manuscript; available in PMC 2017 January 01.

Published in final edited form as:

Biomater Sci. 2016 January ; 4(1): 115–120. doi:10.1039/c5bm00325c.

Cancer cell selective-killing polymer/copper combination†

Huacheng He[a], **Diego Altomare**[a], **Ufuk Ozer**[b], **Hanwen Xu**[a], **Kim Creek**[a], **Hexin Chen**[b], and **Peisheng Xu**[a]

[a]Department of Drug Discovery and Biomedical Sciences, University of South Carolina, Columbia, SC 29208, United States. Fax: 803-777-8356; Tel: 803-777-0075

[b]Department of Biological Sciences, University of South Carolina, Columbia, SC 29208, United States

Abstract

Chemotherapy has been adopted for cancer treatment over decades. However, its efficacy and safety are frequently compromised by the multidrug-resistance of cancer cells and the poor cancer cell selectivity of anticancer drugs. Hereby, we report a combination of pyridine-2-thiol containing polymer and copper which can effectively kill a wide spectrum of cancer cells, including drug resistant cancer cells, while sparing normal cells. The polymer nanoparticle enters cells via an exofacial thiol facilitated route, and releases active pyridine-2-thiol with the help of intracellularly elevated glutathione (GSH). Due to its high GSH level, cancer cells are more vulnerable to the polymer/copper combination. In addition, RNA microarray analysis revealed that the treatment can reverse cancer cells upregulated oncogenes (CIRBP and STMN1) and downregulated tumor suppressor genes (CDKN1C and GADD45B) to further enhance its selectivity for cancer cells.

Introduction

Although various anticancer drugs have been developed to conquer cancer, a large number of cancer patients ultimately still lost their battle against it.[1] There are two major causes for the failure, drug resistance of cancer cells and side effects of anticancer drugs.[2] Because of the inherited or acquired multidrug resistance, cancer cells survive after receiving the original effective drug,[3] which results in the recurrence of the cancer and eventually kills cancer patients. The selectivity of anticancer drugs used in chemotherapy is predominantly relying on the proliferation rate difference between normal cells and cancer cells.[4] Most cancer cells are fast growing.[5] However, besides cancer cells, normal cells in the digestive tract, bone marrow, hair follicles, and reproductive system are also vulnerable to anticancer drugs that targeting quick proliferating cells due to their fast renewal nature. Furthermore, some anticancer drugs even compromise the function of heart, nervous system, and kidneys.

To increase the selectivity of anticancer drug for cancer cells, various approaches have been explored, including utilizing the specific receptors expression level difference between

†Electronic Supplementary Information (ESI) available: Details of synthesis and characterization of polymer, nanoparticles, and cell based *in vitro* assays. See DOI: 10.1039/x0xx00000x

Correspondence to: Peisheng Xu.

normal and cancer cells,[6] as well as the tumor unique physiological properties such as low pH,[7] high GSH,[8] and changed metal ion concentrations.[9] Among them, copper concentration in tumors has attracted extreme high interest recently. Copper is an important trace metal that plays critical roles in maintaining normal biological functions. Elevated copper concentration (up to 2–3 fold) is frequently observed in a wide spectrum of tumors including ovarian, breast, cervical, prostate and leukemia.[10] High copper concentration facilitates tumor angiogenesis. Depletion of copper by copper chelators such as D-penicillamine, trientine, and disulfiram has been proved effective in inhibiting angiogenesis and killing cancer cells both *in vitro* and *in vivo*.[11] Chelators can form complex with copper by thiol, amine, and pyridine ring to reduce copper concentration in the tumor, which eventually result in the death of cancer cells.[12] Thus, several clinic trials involve the copper chelators have been conducted.[13] However, due to the non-specific tissue distribution and rapid clearance of chelators, none or only little beneficial was observed in those trials.

Our preliminary study found that the addition of copper ions to 2, 2′-Dithiodipyridine (DTP) could significantly boost its cytotoxicity for cancer cells and normal cells (Fig. S1). To endow high density of pyridine-2-thiol, the intracellular metabolite of DTP, we designed a poly[(2-(pyridin-2-yldisulfanyl)ethyl acrylate)-co-[poly(ethylene glycol)]] (PDA-PEG) polymer. PDA-PEG was synthesized through free radical polymerization according to our published method.[8] The pyridine rings in PDA can complex with Cu^{2+}, turning the polymer into a multi-chelator system.

Results and discussion

The successful synthesis of the polymer was verified by ^{1}H-NMR (Fig. S2A) and gel permeation chromatography (GPC) (Fig. S2B). The ^{1}H NMR result revealed that the actual ratio between PDA and mPEG in the final PDA-PEG polymer was close to their feeding ratios (1:1). GPC showed that the molecular weight of PDA-PEG polymer was 41.8 kDa. Due to the co-existing of hydrophobic PDA and hydrophilic PEG, the amphiphilic PDA-PEG self-assembles into nanoparticle in aqueous solution. Zeta sizer revealed that PDA-PEG nanoparticles had a hydrodynamic size of 87.64±2.06 nm and carried negative surface charge (−15.4±2.05 mV). The morphology of PDA-PEG nanoparticle was also confirmed by TEM, which showed a spherical shape with a size around 80 nm (Fig. 1A). After the addition of Cu^{2+} ($CuCl_2$, 10 μM), the hydrodynamic size of the nanoparticles increased to 196.4±0.07 nm (Fig. S3), while becoming less negatively charged (−5.47±0.86 mV). Due to the interaction between Cu^{2+} and pyridine ring made the PDA segment more hydrophilic so that the core became less condensed (Fig. 1B), which led to the increase of the particle size.[14] The formation of nanoparticle will endow two advantages for cancer therapy. First, due to the existence of PEG corona, the circulation time of the polymer in the blood stream can be greatly extended. Second, by taking advantage of the leaky structure of the capillaries in the tumor tissue, the formed PDA-PEG/Cu^{2+} nanoparticle can be enriched in the tumor through the so called enhanced permeability and retention (EPR) effect.

To validate whether the polymer form of DTP chelator possesses similar cell killing capacity as its small molecular counterpart, cell proliferation assay was employed in 7 cancer cell lines, 5 normal cell lines, and a NIH 3T3 cell line, an immortalized cell line derived from

normal cells. As expected, PDA-PEG nanoparticle did not show obvious toxicity up to the equivalent DTP concentration of 40 μM for all tested cells (Fig. S4). Similar as DTP, the addition of Cu^{2+} dramatically enhanced the potency of PDA-PEG nanoparticles for cancer cells (Fig. 2). The IC_{50} of PDA-PEG/Cu^{2+} for SKOV-3, NCI/ADR-Res, MDA-MB-231, and UMSCC 22A cells were less than 6 μM (Table S1), and with a IC_{95} less than 20 μM. Contrary to its small molecule counterpart (Fig. S1B), the cell killing effect of PDA-PEG/Cu^{2+} for cancer cells and normal cells are significantly different. Fig. 2 also showed that PDA-PEG/Cu^{2+} combination is non-toxicity to normal cells, including keratinocytes, fibroblasts, breast epithelial cells, colon cells, and hepatocytes, up to 80 μM. The IC_{50}s for normal cells were 10–70 fold higher than those for cancer cells (Table S1). All these suggested that PDA-PEG/Cu^{2+} could selectively kill cancer cells, including drug resistant cancer cells, while sparing normal ones. In addition, Fig. S5 also revealed that the cytotoxicity of PDA-PEG/Cu^{2+} for cancer cells increases with the increase of Cu^{2+} concentration, while not showing influence on normal cells.

To further validate that the PDA-PEG/Cu^{2+} combination can specifically kill cancer cells versus normal ones, NIH 3T3, SKOV-3, NCI/ADR-Res, and UMSCC 22A cells were stained with different color fluorescent dyes. NIH 3T3 cell was selected as a representative normal cell because its comparable growth rate and suitability for co-culture with cancer cells in DMEM medium. Fig. 3 showed that all cells except NIH 3T3 were rounded up after treated with 8.3 μM of PDA-PEG/Cu^{2+}, indicating these cells were not in healthy status. On the contrary, NIH 3T3 cells still kept its original stretched cell shape at 20.79 μM. All these images visually confirmed the MTT results in Fig. 2. This phenomenon was also observed in the multiple cell lines co-culture model (bottom row of Fig. 3), where only NIH 3T3 cells kept their original spindle morphology, indicating that the PDA-PEG/Cu^{2+} combination could selectively kill cancer cells while sparing normal cells in a more disease relevant co-culture model.

To probe the mechanism for PDA-PEG/Cu^{2+} selectively killing cancer cells, we first investigated the cellular uptake of PDA-PEG and PDA-PEG/Cu^{2+} nanoparticle with flow cytometry and confocal microscopy. Fig. 4A showed that the nanoparticles fabricated from Cy5 labeled PDA-PEG and PDA-PEG/Cu^{2+} combination entered cells with identical manners, suggesting that the addition of copper ions did not affect its entering cells. In addition, these nanoparticles showed similar efficiency in entering normal cells (NIH 3T3) and cancer cells (SKOV-3). Therefore, the uptake of PDA-PEG/Cu^{2+} wasn't the reason for its cancer-cell-selectivity. 5,5′-Dithio-bis-(2-nitrobenzoic acid) (DTNB) is a compound binds the free thiol groups on the surface of cell membrane. The addition of DTNB significantly inhibited the cellular uptake of PDA-PEG (Fig. 4B), suggesting that PDA-PEG entering cells via exofacial thiol mediated endocytosis. We think this is because PDA-PEG polymer contains high density of thiol-reactive PDA segment, which can react with exofacial thiols through thiol-disulfide exchange reaction to facilitate cellular uptake. Similar blocking effect was also observed in NIH 3T3 cells treated with DTNB (Fig. S6).

Our previous study found that polymer-drug conjugates linked through disulfide bond could quickly release its payload by cleaving the disulfide bond with the help of intracellular elevated glutathione (GSH).[6] As pyridine-Cu complex analogues had been reported highly

toxic and extensively studied as anticancer drugs, the release of pyridine-Cu complex probably induced cell death.[14] The high cytotoxicity of DTP/copper combination also suggested that pyridine-2-thiol/copper combination could be the active segment for its cytotoxicity. To study the release kinetics of the PDA-PEG/Cu^{2+} nanoparticles, samples were dispersed in phosphate buffers supplemented with different levels of GSH as well as serum containing media to mimic the plasma and intracellular environment. Fig. 5A showed that PDA-PEG/Cu^{2+} is extremely stable at a low reducing environment ([GSH] < 0.1 mM), such as the plasma, where has a GSH level less than 5 μM.[15] However, almost all pyridine-2-thiol segments could be instantly released from PDA-PEG at the GSH level of 10 mM, indicating its super responsiveness to the intracellular reducing condition. Furthermore, the polymer/copper combination was very stable in 50% serum containing medium, only 12.92% pyridine-2-thiol was released after 7 days of incubation (Fig. 5B), suggesting its great stability during blood circulation.

Since there was no significant difference between normal cells and cancer cells in uptaking PDA-PEG/Cu^{2+} nanoparticle, we postulate that the observed cancer-cell-selective-killing effect was due to the intrinsic difference between normal and cancer cells. It has been reported that GSH levels in tumor tissues, such as ovarian, head and neck, breast, and lung cancer are higher than that in normal tissues.[16] To probe whether the high GSH level is also prevail in cancer cells *in vitro*, GSH-Glo™ Glutathione Assay was employed. Interestingly, Fig. 5C revealed that, the GSH level range in normal cells is relatively broad, ranging from 0.48 to 5.65 μM, while most tested cancer cell lines displayed relatively high GSH level (> 2 μM), suggesting that intracellular GSH level could be a valid target for cancer targeted therapy. To prove that, glutathione-monomethylester (GSH-MME, 5 mM) and buthionine sulfoxamine (BSO, 1mM) were employed to boost or deplete the intracellular GSH level in normal cells (NIH 3T3, BNL CL.2, KC, and MCF 10A) or cancer cells (NCI/ADR-Res, HCT 116, UMSCC 22A, SKOV-3, and MDA-MB-231), respectively.[17] After the addition of GSH-MME all normal cells exhibited higher intracellular GSH level (Fig. 5C). As expected, these cells became more vulnerable to the polymer/copper combination treatment (Fig. 5D and S7). On the contrary, BSO treated NCI/ADR-Res, UMSCC 22A, and SKOV-3 cells displayed declined GSH level. Interestingly, only NCI/ADR-Res cells became more tolerant to the polymer/copper combination treatment (Fig. 5E), while the other two cancer cell lines kept their sensitivity to the treatment (Fig. S8). Based on these results shown in Fig. 5, we conclude that intracellular GSH level is not the sole cause for the cancer-cell-selective-killing effect of PDA-PEG/Cu^{2+} nanoparticles.

Among those tested cells, there were several exceptions. First, MCF 10A and KC exhibited higher GSH level than other normal cells and cancer cell, while not sensitive to PDA-PEG/Cu^{2+} treatment. Second, NCI/ADR-Res cells showed lower GSH level than other cancer cells, but still vulnerable to the treatment. Third, SKOV-3 and UMSCC 22A cells displayed lower GSH level after BSO treatment, however, the decreased GSH level only slightly abolished their response to PDA-PEG/Cu^{2+} (Fig. S8). To solve these puzzles, we further investigated the gene response to PDA-PEG/Cu^{2+} treatment in MCF 10A, NCI/ADR-Res, and SKOV-3 cells through RNA microarray analysis. Cells were treated with PDA-PEG/Cu^{2+} for 12 h before the RNA extraction. Microarray analysis data revealed that, for untreated cells, the RNA levels of oncogenes (CIRBP and STMN1) were upregulated, while

tumor suppressor genes (CDKN1C and GADD45B) were downregulated in both ovarian cancer cell lines (Fig. 6A). Surprisingly, PDA-PEG/Cu^{2+} treatment reversed the above gene expression pattern by downregulating the RNA level of CIRBP and STMN1 (>3 folds), while upregulating CDKN1C and GADD45B (>5 folds) (Fig. 6B). Interestingly, no obvious expression level change of these genes was detected in the normal breast cell line. Other studies showed that oncogenes (CIRBP[18] and STMN1[19]) are upregulated while tumor suppressor genes (CDKN1C[20] and GADD45B[21]) are downregulated in various types of cancers. Since the upregulated oncogenes and downregulated tumor suppressor genes stimulate cancer cell proliferation and promote tumor growth, reversing those malregulated genes through PDA-PEG/Cu^{2+} treatment would result in cancer cells apoptosis. For MCF 10A cells, although the high level of GSH could release large amount of pyridine-2-thiol intracellularly, cells still survived due to that those oncogenes and tumor suppressor genes are not sensitive to the treatment. For NCI/ADR-Res cells, whose GSH level is relatively low but still high enough to release needed pyridine-2-thiol to regulate their oncogenes and tumor suppressor genes due to its high sensitivity. Similarly, BSO decreased the GSH level in SKOV-3 and UMSCC 22A cells, while the resulted GSH level is still high enough to release pyridine-2-thiol to regulate their oncogenes and tumor suppressor genes. Therefore, the cancer-cell-selective-killing property of PDA-PEG/Cu^{2+} is the combination effects of high intracellular GSH level and the malregulation of oncogenes and tumor suppressor genes in cancer cells.

CDKN1C is an inhibitor for G1 cyclin/Cdk complexes and causes cell arrest in G1 phase.[20] To investigate the effect of CDKN1C up-regulation after PDA-PEG/Cu^{2+} treatment, cell cycle analysis was employed. Fig. 7 showed that PDA-PEG/Cu^{2+} inhibited cell division and arrested cancer cells in G1 phase, which could induce cell apoptosis. As expected, PDA-PEG polymer or Cu^{2+} ion alone did not show any effect on the cell cycle distribution of SKOV-3 cells.

Conclusions

In summary, we developed a cancer-cell-selective-killing nanoparticle from PDA-PEG/Cu^{2+} combination aiming for safe and effective cancer therapy. The polymer/Cu^{2+} based nanoparticle entered cells through the interaction with exofacial thiols, and subsequently released pyridine-2-thiol-Cu complex to kill cells. Due to the difference in the intracellular GSH level as well as the expression level of oncogenes (CIRBP and STMN1) and tumor suppressor genes (CDKN1C and GADD45B) between normal and cancer cells, the PDA-PEG/Cu^{2+} exhibited high selectivity in killing a broad spectrum of cancer cells, including drug resistant one, while sparing normal cells. Therefore, PDA-PEG/Cu^{2+} nanoparticle will provide a new paradigm for the cure of ovarian and other cancers. The ongoing research will investigate the cell killing mechanism of PDA-PEG/Cu^{2+} in molecular level and test whether the cancer-cell-selective-killing effect of PDA-PEG/Cu^{2+} can be translated into a safe and effective cancer treatment tool *in vivo*.

Supplementary Material

Refer to Web version on PubMed Central for supplementary material.

Acknowledgments

The authors want to thank the ASPIRE award from the Office of the Vice President for Research of The University of South Carolina and National Institutes of Health (5P20GM109091-02 and 1R15CA188847-01A1) for financial support of the research.

Notes and references

1. Siegel R, Ma J, Zou Z, Jemal A. CA Cancer J Clin. 2014; 64:9–29. [PubMed: 24399786]
2. Holohan C, Van Schaeybroeck S, Longley DB, Johnston PG. Nat Rev Cancer. 2013; 13:714–726. [PubMed: 24060863] Liang, X-J.; Chen, C.; Zhao, Y.; Wang, P. Multi-Drug Resistance in Cancer. Zhou, J., editor. Vol. 596. Humana Press; 2010. p. 467-488.ch 21
3. Pauwels EK, Erba P, Mariani G, Gomes CM. Drug News Perspect. 2007; 20:371–377. [PubMed: 17925891]
4. Masui K, Gini B, Wykosky J, Zanca C, Mischel PS, Furnari FB, Cavenee WK. Carcinogenesis. 2013; 34:725–738. [PubMed: 23455378]
5. Herst PM, Davis JE, Neeson P, Berridge MV, Ritchie DS. Haematologica. 2009; 94:928–934. [PubMed: 19535345] Mitchison TJ. Mol Biol Cell. 2012; 23:1–6. [PubMed: 22210845]
6. He H, Cattran AW, Nguyen T, Nieminen AL, Xu P. Biomaterials. 2014; 35:9546–9553. [PubMed: 25154666] Remant BK, Chandrashekaran V, Cheng B, Chen H, Pena MM, Zhang J, Montgomery J, Xu P. Mol Pharm. 2014; 11:1897–1905. [PubMed: 24779647]
7. Ling D, Park W, Park S-j, Lu Y, Kim KS, Hackett MJ, Kim BH, Yim H, Jeon YS, Na K, Hyeon T. J Am Chem Soc. 2014; 136:5647–5655. [PubMed: 24689550] Ding, H-m; Ma, Y-q. Sci Rep. 2013; 3:2804. [PubMed: 24076598]
8. Bahadur RKC, Xu P. Adv Mater. 2012; 24:6479–6483. [PubMed: 23001909] Cheng B, Thapa B, RKC, Xu P. J Mater Chem B. 2015; 3:25–29.
9. Gupte A, Wadhwa S, Mumper RJ. Bioconjug Chem. 2008; 19:1382–1388. [PubMed: 18570451] Gupte A, Mumper RJ. Free Radic Biol Med. 2007; 43:1271–1278. [PubMed: 17893040]
10. Gupte A, Mumper RJ. Cancer Treat Rev. 2009; 35:32–46. [PubMed: 18774652]
11. Wang F, Jiao P, Qi M, Frezza M, Dou QP, Yan B. Curr Med Chem. 2010; 17:2685–2698. [PubMed: 20586723] Chen D, Dou QP. Expert Opin Ther Targets. 2008; 12:739–748. [PubMed: 18479220]
12. Lewis DJ, Deshmukh P, Tedstone AA, Tuna F, O'Brien P. Chem Comm. 2014; 50:13334–13337. [PubMed: 25233190] Santini C, Pellei M, Gandin V, Porchia M, Tisato F, Marzano C. Chem Rev. 2013; 114:815–862. [PubMed: 24102434]
13. Brem S, Grossman SA, Carson KA, New P, Phuphanich S, Alavi JB, Mikkelsen T, Fisher JD. f. t. N. A. t. B. T. T. C. Consortium. Neuro Oncol. 2005; 7:246–253. [PubMed: 16053699] Schweizer MT, Lin J, Blackford A, Bardia A, King S, Armstrong AJ, Rudek MA, Yegnasubramanian S, Carducci MA. Prostate Cancer Prostatic Dis. 2013; 16:357–361. [PubMed: 23958896]
14. Kinoshita I, James Wright L, Kubo S, Kimura K, Sakata A, Yano T, Miyamoto R, Nishioka T, Isobe K. Dalton Trans. 2003:1993–2003.
15. Anderson ME. Methods Enzymol. 1985; 113:548–555. [PubMed: 4088074]
16. Gamcsik MP, Kasibhatla MS, Teeter SD, Colvin OM. Biomarkers. 2012; 17:671–691. [PubMed: 22900535]
17. Xu P, Quick GK, Yeo Y. Biomaterials. 2009; 30:5834–5843. [PubMed: 19631979]
18. Sakurai T, Kashida H, Watanabe T, Hagiwara S, Mizushima T, Iijima H, Nishida N, Higashitsuji H, Fujita J, Kudo M. Cancer Res. 2014; 74:6119–6128. [PubMed: 25187386] Sakurai T, Yada N, Watanabe T, Arizumi T, Hagiwara S, Ueshima K, Nishida N, Fujita J, Kudo M. Cancer Sci. 2015; 106:352–8. [PubMed: 25611373]
19. Akhtar J, Wang Z, Yu C, Li CS, Shi YL, Liu HJ. BMC Cancer. 2014; 14:28. [PubMed: 24433541] Batsaikhan BE, Yoshikawa K, Kurita N, Iwata T, Takasu C, Kashihara H, Shimada M. Anticancer Res. 2014; 34:4217–4221. [PubMed: 25075050]
20. Kavanagh E, Joseph B. Biochim Biophys Acta. 2011; 1816:50–56. [PubMed: 21447370] Borriello A, Caldarelli I, Bencivenga D, Criscuolo M, Cucciolla V, Tramontano A, Oliva A, Perrotta S, Della Ragione F. Mol Cancer Res. 2011; 9:1269–1284. [PubMed: 21816904]

21. Zhang L, Yang Z, Liu Y. Exp Biol Med (Maywood). 2014; 239:773–778. [PubMed: 24872428]
Tamura RE, de Vasconcellos JF, Sarkar D, Libermann TA, Fisher PB, Zerbini LF. Curr Mol Med. 2012; 12:634–651. [PubMed: 22515981]

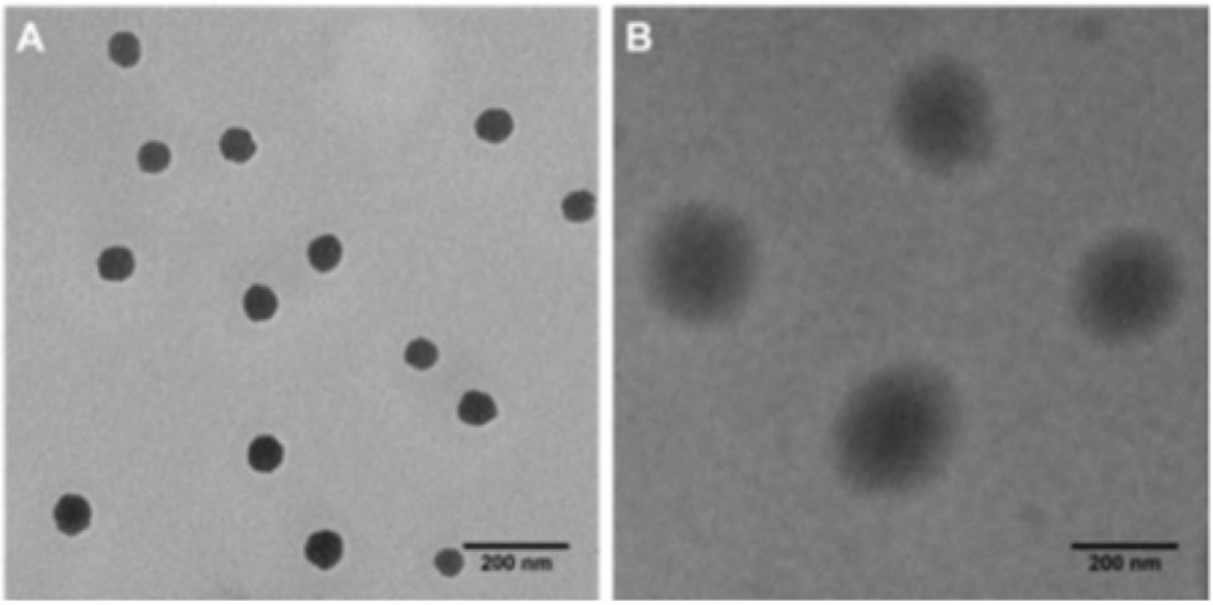

Fig. 1.
TEM images of nanoparticle fabricated from PDA-PEG alone (A), and PDA-PEG/Cu^{2+} combination (B). Scale bars are 200 nm.

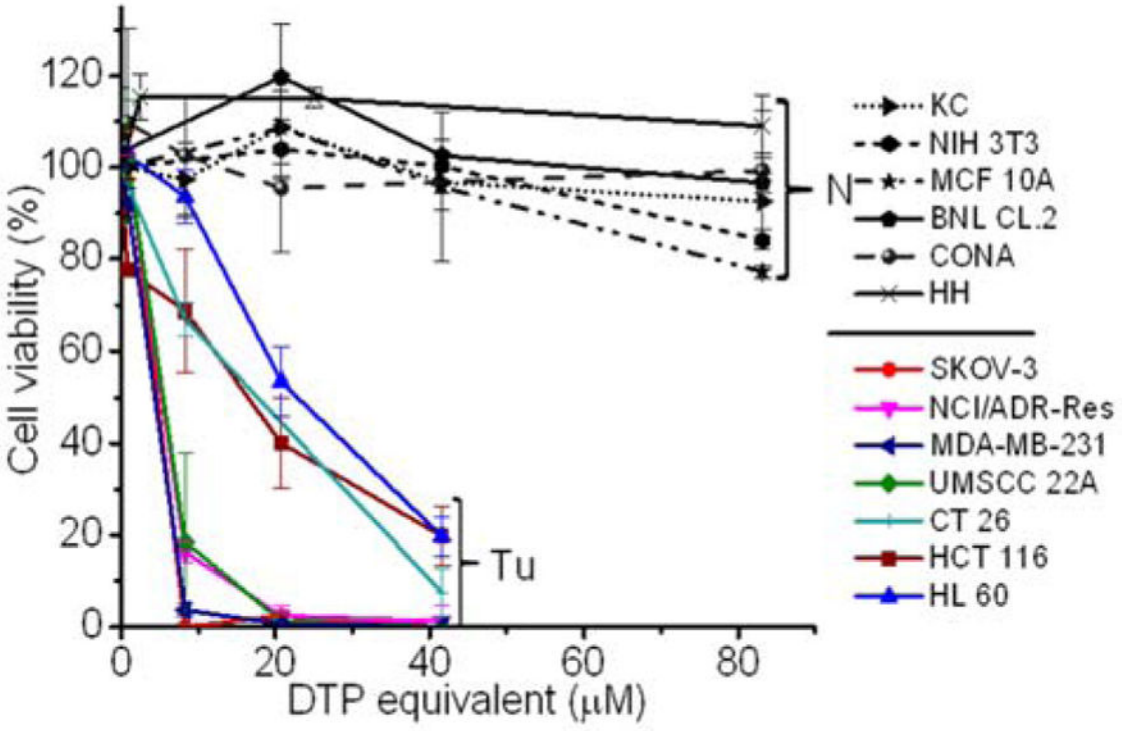

Fig. 2.

Cytotoxicity of PDA-PEG/Cu^{2+} combination for normal (N) and cancer (Tu) cells. Normal cells include KC (human keratinocyte), NIH 3T3 (murine fibroblast), MCF 10A (human breast epithelial cell), BNL CL.2 (murine liver cell), CONA (CCD 841 CoN, human colon cell), and HH (human hepatocyte). Data represent the means±SD, n=3.

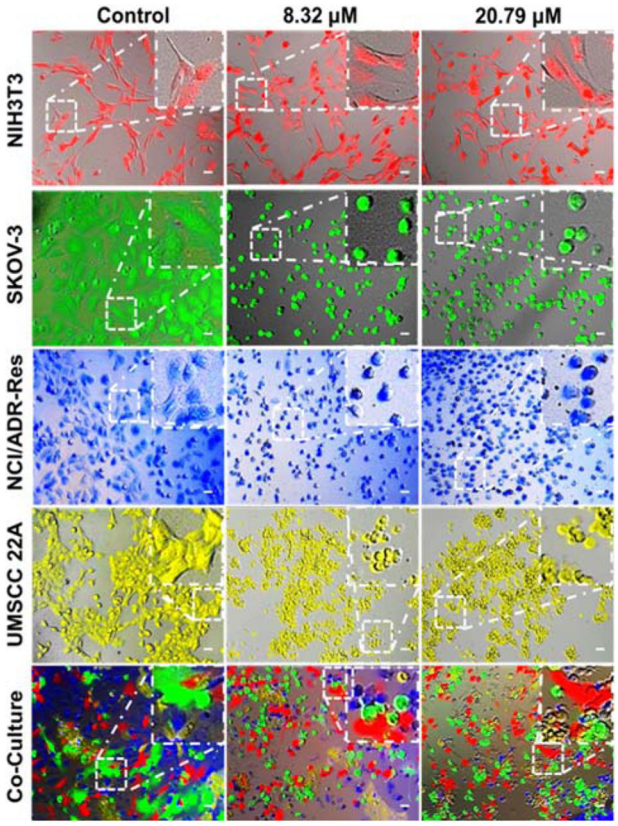

Fig. 3.

Fluorescence images of cancer cells after culturing with different concentrations of PDA-PEG/Cu^{2+} combination. NIH 3T3, NCI/ADR-Res, SKOV-3 and UMSCC 22A were pre-stained with Cell Tracker™ deep red, blue, green CMFDA and orange CMTMR dye, respectively, and imaged 24 h after the treatment. The scale bars were 40 μm.

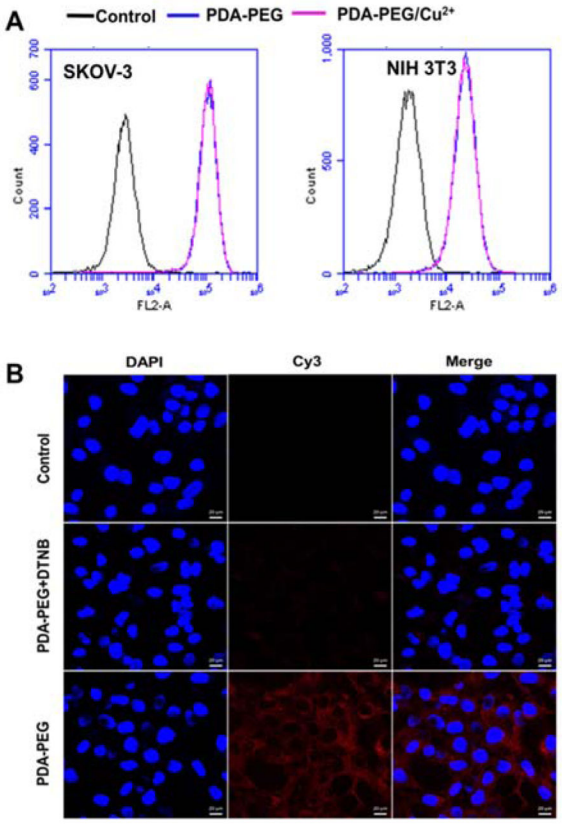

Fig. 4.

Flow cytometry spectra of SKOV-3 and NIH 3T3 cells (A) and confocal images of cellular uptake of nanoparticles in SKOV-3 cells (B). Cellular uptake assays were carried out 1 h after the addition of nanoparticles. Scale bars were 20 μm.

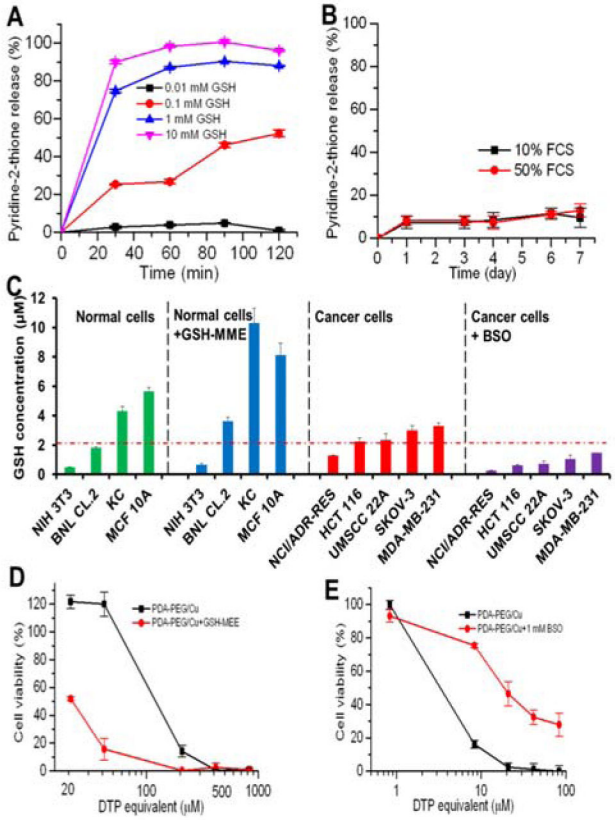

Fig. 5.

The release kinetic of pyridine-2-thiol liberating from PDA-PEG at different GSH levels (A) and in serum containing media (B), the GSH level in different cell lines and response to the addition of GSH-MME and BSO (C), GSH-MME effect on the cytotoxicity of PDA-PEG/Cu^{2+} for MCF10A cells (D), and BSO effect on the cytotoxicity of PDA-PEG/Cu^{2+} combination for NCI/ADR-Res cells (E). Data represent the means±SD, n=3.

A

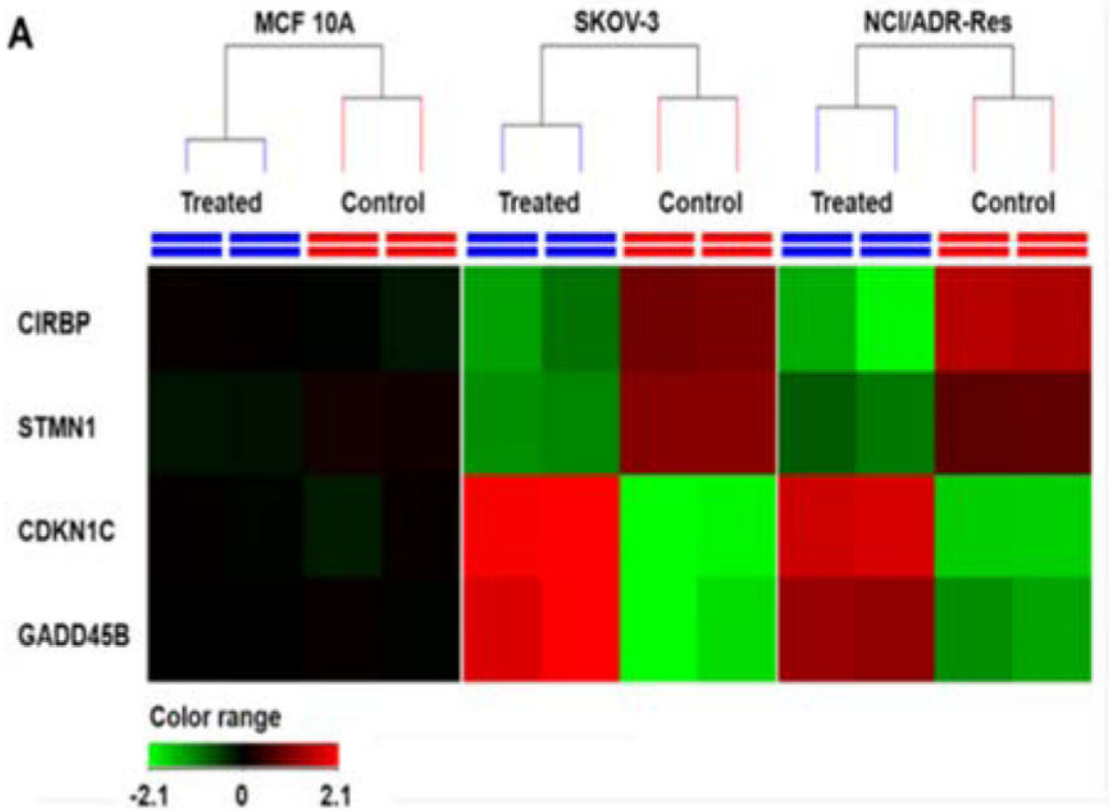

B

	SKOV-3	NCI/ADR-Res	MCF10A
Oncogene	Fold of change		
CIRBP	4.25 ↓	9.04 ↓	1.11 ↓
STMN1	4.74 ↓	3.10 ↓	1.22 ↓
Tumor suppressor gene			
CDKN1C(p57)	20.55 ↑	10.72 ↑	1.06 ↑
GADD45B	16 ↑	5.45 ↑	1.01 ↑

Fig. 6.

RNA expression in response to PDA-PEG/Cu^{2+} treatment. Cells were treated with 41.58 μM of PDA-PEG/Cu^{2+} for 12 h. (A) Heatmap RNA level with and without drug treatment. Red: upregulation; green: downregulation; black: no change. (B) Genes alteration fold after treatment.

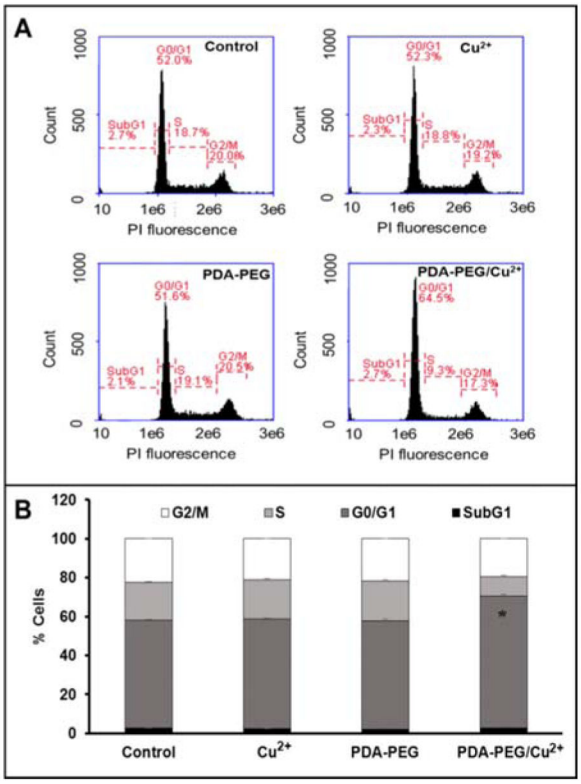

Fig. 7.

Cell cycle analysis of SKOV-3 cells after treated with 41.58 μM of PDA-PEG/Cu2+ for 12 h. Flow cytometry spectra (A) and quantitive analysis (B) of cell cycle. Data represent the means±SD, n=3. *p<0.01.